Published in final edited form as:
Mol Pharm. 2013 May 6; 10(5): 1977–1987. doi:10.1021/mp4000019.

Polymeric Curcumin Nanoparticle Pharmacokinetics and Metabolism in Bile Duct Cannulated Rats

Peng Zou[1], **Lawrence Helson**[2], **Anirban Maitra**[3], **Stephan T. Stern**[1,*], and **Scott E. McNeil**[1]

[1]Nanotechnology Characterization Laboratory, Advanced Technology Program, SAIC-Frederick, Inc., NCI-Frederick, Frederick, MD 21702

[2]Sign Path Pharma, Inc, 1375 California Road, Quakertown, PA 18951

[3]Johns Hopkins University School of Medicine, 1550 Orleans Street, Baltimore, MD 21231

Abstract

The objective of this study was to compare the pharmacokinetics and metabolism of polymeric nanoparticle encapsulated (nanocurcumin), and solvent solubilized curcumin formulations in Sprague Dawley (SD) rats. Nanocurcumin is currently under development for cancer therapy. Since free, unencapsulated curcumin is rapidly metabolized and excreted in rats, upon i.v. administration of nanocurcumin only nanoparticle encapsulated curcumin can be detected in plasma samples. Hence, the second objective of this study was to utilize the metabolic instability of curcumin to assess *in vivo* drug release from nanocurcumin. Nanocurcumin and solvent solubilized curcumin were administered at 10 mg curcumin/kg by jugular vein to bile duct-cannulated male SD rats (n = 5). Nanocurcumin increased the plasma C_{max} of curcumin 1749 fold relative to the solvent solubilized curcumin. Nanocurcumin also increased the relative abundance of curcumin and glucuronides in bile, but did not dramatically alter urine and tissue metabolite profiles. The observed increase in biliary and urinary excretion of both curcumin and metabolites for the nanocurcumin formulation suggested rapid, “burst” release of curcumin. Although the burst release observed in this study is a limitation for targeted tumor delivery, nanocurcumin still exhibits major advantages over solvent solubilized curcumin, as the nanoformulation does not result in the lung accumulation observed for the solvent solubilized curcumin and increases overall systemic curcumin exposure. Additionally, the remaining encapsulated curcumin fraction following burst release is available for tumor delivery via the enhanced permeation and retention effect commonly observed for nanoparticle formulations.

*Address correspondence to: Stephan T. Stern, PhD, DABT, Nanotechnology Characterization Laboratory, Advanced Technology Program, SAIC-Frederick, Inc., NCI-Frederick, Frederick, MD 21702, Phone: 301-846-6198, Fax: 301-846-6399, sternstephan@mail.nih.gov.

Conflict of Interest Disclosure The content of this publication does not necessarily reflect the views or policies of the Department of Health and Human Services, nor does mention of trade names, commercial products, or organizations imply endorsement by the U.S. Government.

Supporting Information Supplemental tables and figures are included separately as Supporting Information. Supplemental tables, Tables S1–S5, contain bioanalytical methods utilized in the pharmacokinetic studies. These tables include the mass spectrometry parameters for analytes (Table S1), limits of quantification (LOQ) for the analytes in tissue matrices (Table S2), calibration standards for analytes in tissue matrices (Table S3), precision, accuracy and recovery of curcumin in tissue matrices (Table S4), and precision, accuracy and recovery of tetrahydrocurcumin, hexahydrocurcumin and vanillylidenacetone in tissue matrices (Table S5). Supplemental figures, Figures S1–S4, include the curcumin degradation pathways and in vitro stability studies (Figure S1), nanocurcumin physicochemical characterization data (hydrodynamic size and zeta potential) (Figure S2), evaluation of curcumin aggregation in plasma (Figure S3), and validation studies for curcumin-glucuronide hydrolysis by β-glucuronidase (Figure S4). This material is available free of charge via the Internet at http://pubs.acs.org

Keywords

curcumin; nanoformulation; metabolite profile; biliary excretion; urinary excretion

Introduction

Nanoformulations, such as polymeric nanoparticles and liposomes, have been successfully used to increase the solubility and metabolic stability of water-insoluble drugs, thus increasing systemic exposure. Encapsulation of drug molecules in polymeric nanoparticles and liposomes has been shown to significantly reduce the apparent clearance and prolong the apparent circulation half-life compared with unformulated drugs[1]. Due to the unique biodistribution characteristics of nanoparticles, e.g., mononuclear phagocytic system (MPS) uptake and enhanced permeability and retention (EPR) effect, nanoformulations may also alter absorption, distribution, metabolism, and excretion (ADME) of encapsulated drugs[2].

The effects of liposomal formulation on distribution, metabolism, and excretion of encapsulated drugs are well established[3–5]. For example, compared with free doxorubicin, intravenously (i.v.) administered liposomal doxorubicin exhibited slower elimination, higher uptake into liver and spleen, and lower uptake into kidney, heart, and lung in rats[4]. Liposomal formulation also reduced both biliary and urinary excretion of doxorubicin, and increased the relative excretion of metabolites. Similarly, encapsulating 5-fluoro-2′-deoxyuridine into liposomes decreased biliary excretion[5]. Liposomal formulation of gadolinium (Gd), a magnetic resonance imaging (MRI) contrast agent, changed the predominant elimination pathways in rats[3]. Unlike free Gd contrast agents, liposomal Gd was eliminated mainly through the biliary, instead of the renal system. Pharmacokinetic studies of polymeric nanoparticle-entrapped drugs have primarily focused on plasma profiles and biodistribution[6, 7], with effects on metabolite profiles, and biliary and urinary excretion of entrapped drugs less well characterized[8].

Curcumin is a natural diphenolic compound derived from turmeric (*Curcuma longa*), which is currently undergoing evaluation as a chemopreventive and anticancer agent[9]. In established cancers, curcumin principally acts as a chemosensitizer, improving the combinatorial efficacy with conventional cytotoxic agents, like gemcitabine and doxorubicin[10, 11]. Curcumin's clinical application has thus far been limited by low solubility, low bioavailability, rapid metabolism and degradation at physiological pH[10]. While curcumin is stable under acidic conditions, and plasma proteins can stabilize curcumin at physiological pH, it rapidly degrades to vanillin, ferulic acid, and vanillylidenacetone at pH ≥ 6.8 (Fig. S1A)[12]. In animal models, curcumin is rapidly metabolized into tetrahydrocurcumin (THC) and hexahydrocurcumin (HHC), and their sulfate and glucuronide conjugates (Fig. 1), which are excreted into bile and urine[13, 14]. Numerous curcumin nanoformulations have been developed to increase oral absorption, systemic exposure (AUC, C_{max}) and mean residence time (MRT) of entrapped curcumin[10, 15–19]. However, it is still unknown if the nanoformulations can alter the metabolite profile or excretion pathways of curcumin. Altered metabolism resulting from curcumin nanoformulation could be important in light of the fact that some studies have suggested that certain metabolites, such as THC and phenolic glucuronides, are biologically active and may be responsible for at least some of the pharmacology attributed to curcumin[20, 21].

Drug release kinetics is one of the critical factors which determine ADME of nanoformulated drugs. Targeted drug delivery systems require controlled and sustained release kinetics. The release kinetics of nanoformulated drugs are usually evaluated using in

vitro release assays. However, traditional in vitro release assays have been demonstrated to be a poor predictor of in vivo release. Nanoformulated drugs exhibiting sustained in vitro release have been found to be rapidly released in vivo[22]. Furthermore, it is difficult to measure *in vivo* drug release kinetics since most current sample preparation methods (e.g., liquid-liquid extraction, solid phase extraction, and protein precipitation) cannot accurately distinguish encapsulated drug vs. free drug in blood and tissue matrices. Due to metabolic instability, free, unecapsulated curcumin released from nanoformulations in vivo is rapidly metabolized and excreted, with encapsulated curcumin accounting for the majority of total curcumin measured in vivo. Curcumin and metabolites, therefore, can be used to estimate nanoparticle encapsulated and unencapsulated fractions, respectively, allowing assessment of *in vivo* drug release without requiring bioanalytical methods that can distinguish encapsulated and unencapsulated drug.

The objectives of this study were to: 1) determine the effects of polymeric nanoparticle encapsulation (nanocurcumin) on the metabolite profile, excretion, and tissue distribution of curcumin; 2) assess the in vivo release of curcumin from nanocurcumin. The pharmacokinetic and metabolic profiles, biliary and urinary excretion, and tissue distribution of nanocurcumin and solvent solubilized curcumin were evaluated in bile duct-cannulated rats. Additionally, *in vivo* release of curcumin from nanocurcumin was assessed by quantifying both curcumin and metabolites in plasma, tissues, bile, urine, and feces.

Experimental

Materials

High purity synthetic curcumin (>99%) was purchased from Axxora (Farmingdale, NY). Curcumin-glucuronide was purchased TLC PharmaChem (Vaughan, Canada). Tetrahydrocurcumin (THC), hexahydrocurcumin (HHC), bisdemethoxycurcumin, vanillylidenacetone, β-glucuronidase from *Escherichia coli* (5 million units/g protein), sulfatase from *Helix pomatia* (sulfatase > 10,000 units/g protein, β-glucuronidase > 300,000 units/g protein), monomers and reagents for polymer nanoparticle synthesis, specifically N-isopropylacrylamide (NIPAAM), vinylpyrrolidone (VP), acrylic acid (AA), N, N′-methylenebis-acrylamide, ammonium persulfate, and ferrous sulfate were obtained from Sigma (St. Louis, MO). MI-129 was a gift from Dr. Shaomeng Wang, University of Michigan. BD Vacutainer, PTS gel lithium heparin plus blood collection tubes were purchased from Moore Medical (New Britain, CT). Formic acid (LC-MS grade), acetonitrile (LC-MS grade), and ammonium acetate were purchased from Fisher Scientific (Pittsburgh, PA). Filter units (0.2 μm pore size) were obtained from Millipore (Billerica, MA).

Polymeric Nanoparticle Formulation and Characterization

Polymeric nanoparticles composed of NIPAAM, VP, and AA were synthesized through a free radical reaction according to the previously described method. Curcumin was loaded into the nanoparticles as described previously[23]. A Zetasizer Nano ZS instrument (Malvern Instruments, Southborough, MA) with a backscattering detector was used for measuring the hydrodynamic size (diameter) at 25°C in a low-volume quartz cuvette. Hydrodynamic size is reported as the intensity-weighted average. The stock solution of curcumin-loaded nanoparticles (nanocurcumin) was diluted in phosphate buffered saline (PBS) to give a final concentration of 1 mg polymer/mL and the solution was filtered through a 0.2 μm filter. A minimum of 12 measurements were taken for each sample. The Zetasizer Nano ZS instrument was also used to measure the zeta potential of nanocurcumin. Nanocurcumin was diluted in 10 mM NaCl (pH 7.3) to give a 1 mg polymer/mL final nanoparticle concentration. The sample were then loaded into a folded capillary flow cell and a voltage of 100 V was applied. A minimum of three measurements were taken. To determine the

loading capacity of curcumin, nanocurcumin was suspended in acetonitrile (containing 0.1% formic acid) at a polymer concentration of 1 mg/mL. The solution was sonicated for 1 min and centrifuged (14000 rpm × 10 min). The supernatant was injected into the HPLC to measure the amount of curcumin by the method below.

Stability Assay

Nanocurcumin and curcumin stock solutions were diluted in PBS, citric acid-adjusted PBS buffer (PBS pH was adjusted to 5.7 using citric acid) and rat plasma in triplicate to give a final curcumin concentration of 2 μg/mL. The solutions (1 mL) were incubated at 37°C for 1 h and an aliquot of 50 μL of solution was collected at 0, 5, 10, 15, 30, 45, and 60 min. Protein was precipitated with 150 μL of ice-cold acetonitrile containing an internal standards, bisdemethoxycurcumin (500 ng/mL) and MI-129 (500 ng/mL). The samples were centrifuged at 14,000 rpm for 10 min and 10 μL of supernatant was analyzed by the LC-VIS-MS method below.

To assess the stability of curcumin in dosing solutions of nanocurcumin (equivalent to 2.5 mg curcumin/mL in PBS) and solvent solubilized curcumin (5 mg/mL in DMSO/PBS 1:1 (v/v)), an aliquot of both dosing solutions was kept at room temperature for 48 h. The degradation of curcumin was monitored by the LC-Vis-MS method below. To ensure DMSO/PBS curcumin did not aggregate in plasma, curcumin dosing solution (5 mg/mL) was diluted 10, 20, and 50-fold with rat plasma. The particle size of possible aggregates was measured in triplicate by the Zetasizer Nano ZS method above.

Pharmacokinetic Studies

NCI-Frederick is accredited by the Association for Assessment and Accreditation of Laboratory Animal Care International and follows the U.S. Public Health *Service Policy for the Care and Use of Laboratory Animals*. Animal care was provided in accordance with the procedures outlined in the *Guide for the Care and Use of Laboratory Animals* (National Institutes of Health, 1996). Twelve double jugular catheterized and bile duct cannulated male Sprague-Dawley (SD) rats (65 days old, approximate weight of 300 g) were purchased from Charles River Laboratories, Inc. (Raleigh, NC). The animals were placed in metabolic cages, fed standard rat food (Purina) and chlorinated tap water *ad libitum*. The animal rooms were maintained on a 12-h light/dark cycle, with a temperature range between 20° and 22°C, and 50% relative humidity.

Dosing solutions of nanocurcumin and solvent solubilized curcumin were freshly prepared and 10 mg curcumin/kg was administered via the left jugular vein catheter (n = 5). A blank control group (n = 2) was treated with PBS (4 mL/kg). Blood samples (300 μL) were collected via the right jugular catheters at each time point (15 min, and 1, 2, 4, 8, 24, and 30 h postdose) and placed in lithium heparinized tubes. The blood was centrifuged (2000 g for 10 min) immediately to collect plasma. Bile samples were collected at 1 h increments for the first 8 h. Urine and feces were collected at 8 and 24 h intervals. Replacement saline was given subcutaneously (s.c.) for bile removed. All samples were weighed, frozen at −80°C, and protected from light.

Tissue Distribution Studies

Thirteen single jugular catheterized male Sprague-Dawley (SD) rats (65 days old) were randomly divided into 5 groups. Group 1 (n =3) and group 2 (n =3) were administered nanocurcumin (equivalent to 10 mg curcumin/kg), while group 3 (n =3) and group 4 (n =3) were administered solvent solubilized curcumin (10 mg/kg) via the jugular vein catheter. Group 5 (n = 1) received PBS i.v. (4 mL/kg). The blood and tissue collection time point for groups 1, 3 and 5 was at 15 min and for groups 2 and 4 was 60 min. At each collection time

point, rats were euthanized by CO_2 asphyxiation. Blood (1 mL) was collected in Li-heparinized tubes from cardiac puncture and spun (2000 g for 10 min) to collect plasma. Liver, lungs, kidneys, heart and spleen were collected, washed in ice cold pH 5.7 citric acid-PBS buffer, blotted dry, weighed, and frozen at −80°C.

Sample Preparation

Plasma—β-glucuronidase and sulfatase stock solutions were prepared in pH 5.7 citric acid-PBS buffer at concentrations of 50,000 units/mL and 1000 units/mL, respectively. Rat plasma sample (40 μL aliquots) and 3 μL of 0.25 M citric acid were added to each microcentrifuge tube in triplicate. An aliquot (7 μL) of β-glucuronidase solution or sulfatase solution was added to the three tubes. After incubation at 37°C for 1 h, the samples were mixed with 150 μL of ice-cold acetonitrile containing 0.1% formic acid and two internal standards, bisdemethoxycurcumin (500 ng/mL) and MI-129 (500 ng/mL). The samples were placed in a freezer (−20 °C) for 10 min and then centrifuged at 14,000 rpm for 10 min at 4°C. The supernatants were analyzed by the LC-Vis-MS method below.

Urine—Rat urine sample (50 μL aliquots) and 3 μL of 0.5 M citric acid were added to each microcentrifuge tube in triplicate. An aliquot (7 μL) of β-glucuronidase solution or sulfatase solution was added to the three tubes. After incubation at 37°C for 1 h, the samples were mixed with 180 μL of ice-cold acetonitrile containing 0.1% formic acid and internal standards. Similar procedures described above for plasma samples were applied to urine samples.

Bile—Rat bile sample (60 μL aliquots) and 10 μL of 0.1 M citric acid were added to each microcentrifuge tube in triplicate. An aliquot (10 μL) of β-glucuronidase solution or sulfatase solution was added to the three tubes. After incubation at 37°C for 1 h, the samples were mixed with 240 μL of ice-cold acetonitrile containing 0.1% formic acid and internal standards. Similar procedures described above for plasma samples were applied to bile samples.

Feces—Feces were mixed with acetonitrile containing 0.1% formic acid and internal standards to a concentration of 0.1 g/mL. The mixture was vortexed until the feces were homogenized, sonicated for 5 min, then centrifuged 4000 rpm for 10 min. Supernatant (0.5 mL) was evaporated in a microcentrifuge tube to dryness under nitrogen in triplicate, and the residue was dissolved in pH 5.7 citric acid-PBS buffer (50 μL). An aliquot (10 μL) of β-glucuronidase solution or sulfatase solution was added to the three tubes. After incubation at 37°C for 1 h, the samples were mixed with 180 μL of ice-cold acetonitrile containing 0.1% formic acid. Similar procedures described above for plasma samples were applied to feces samples.

Tissues—Tissue samples were accurately weighed and homogenized in four volumes (w/v) of pH 5.7 citric acid-PBS buffer using a Polytron PT1300D homogenizer (Kinematica, Inc., Bohemia, NY). Tissue homogenate (50 μL) and 3 μL of 0.25 M citric acid were added to each microcentrifuge tube in triplicate. An aliquot (7 μL) of β-glucuronidase solution or sulfatase solution was added to the three tubes. After incubation at 37°C for 1 h, the samples were mixed with 180 μL of ice-cold acetonitrile containing 0.1% formic acid and two internal standards. Similar procedures described above for plasma samples were applied to bile samples.

Validation of enzymatic hydrolysis—To ensure efficient and complete hydrolysis of conjugates, curcumin-glucuronide standard was spiked into blank plasma, urine, bile, feces and tissue homogenates at 40 μg/mL and 100 μg/mL and incubated with β-glucuronidase or

sulfatase (containing β-glucuronidase > 300,000 units/g) as described above. After incubation, the remaining curcumin-glucuronide and formed curcumin were quantified. Since curcumin-sulfate standard is not commercially available, the validation of sulfate hydrolysis was not conducted. The complete hydrolysis of sulfates was confirmed by the disappearance of the chromatographic peaks identified as sulfates in unknown samples.

LC-Vis-MS analysis

LC-Vis-MS analysis was performed using an LC-MS 2020 system equipped with a UV/Vis detector (Shimadzu, Columbia, MD). Separation was performed on a Zorbax SB-C18 column of the dimensions 4.6 × 150 mm and a particle size of 5 μm (Agilent) coupled with a guard column (4.6 × 12.5 mm). The analytes (injection volume 10 μL) were separated by a binary gradient at a flow rate of 1 mL/min of 10 mM ammonium acetate containing 0.1% formic acid as solvent A and acetonitrile containing 0.1% formic acid as solvent B. For plasma, urine and tissue sample analysis, the following linear gradients were used: 0 min, 30% B; 3 min, 30% B; 11 min, 60% B; 13 min, 60% B; 13.5 min, 90% B; 15 min, 90% B; 15.01 min, 30% B; and 19 min, 30% B. For bile sample analysis, the following gradient was used: 0 min, 30% B; 3 min, 30% B; 18 min, 55% B; 20 min, 90% B; 20.01 min, 30% B; and 24 min, 30% B. Column temperature and sample temperature were maintained at 30 and 4°C, respectively. Curcumin and curcumin glucuronide were detected using a UV/Vis detector operating at 425 nm, and bisdemethoxycurcumin served as an internal standard (IS) for LC-UV/Vis analysis. THC, HHC and vanillylidenacetone were detected using positive ESI MS in selected ion monitoring mode and MI-129 was used as an IS for LC-MS analysis. MS parameters for THC, HHC, and vanillylidenacetone were optimized by injecting 10 μg/mL of analyte solutions and shown in the supplemental table (Table S1).

Calibration and Method Validation

Calibration standards for each analyte were prepared in tissue, plasma, bile, urine, and feces matrices from naive untreated rats. The calibration standards in each matrix were worked up for LC-Vis-MS analysis in the exact procedures as described for the unknown samples. An equivalent amount of IS was added to both unknown samples and calibration standards before LC-Vis-MS analysis. Blank samples were interspersed in the sequence to ensure no inter-sample carryover was occurring. LC-UV/Vis and LC-MS methods were validated for LOQs, linearity of calibration curves, specificity, precision, accuracy, and recovery in various matrices. For each analyte, the LOQ values were determined using signal-to-noise (S/N) = 10. See Table S2 for the LOQ values of curcumin, THC, HHC, and vanillylidenacetone in various matrices. The linearity ranges of calibrations curves are shown in Table S3. The precision and accuracy of the methods were determined by repeated analysis of the quality control samples (QCs) prepared from a separate stock solution at low, medium and high concentrations. The precision of the methods was evaluated by the relative standard deviations (RSD) with replicate assays (n =5), and the accuracy of the methods was evaluated based on the error of the assayed QCs (n =3) relative to their spiked concentrations (RE).To determine extraction recovery, blank sample and post-extracted blank sample were spiked with analytes at three concentrations (n = 3). The results of precision, accuracy, and extraction recovery in various matrices were shown in Table S4 and Table S5.

Data Analysis

For each analyte, three concentrations were determined: the concentration without sample hydrolysis (C1), the concentration after hydrolysis of glucuronides (C2), and the concentration after hydrolysis of both sulfates and glucuronides (C3). The total concentration of curcumin glucuronides was calculated as C2 - C1, while the total concentration of sulfates and sulfate/glucuronide dual conjugates was calculated as C3 – C2.

The concentrations of THC and HHC conjugates were calculated following the same procedures. The concentrations of curcumin and its metabolites were presented as ng/mL or percentage of injected dose (%ID). The %ID of curcumin in plasma, bile and urine was calculated as: (curcumin concentration × volume of plasma, bile or urine)/total dose × 100%. The %ID of curcumin in tissues was calculated as: (tissue curcumin concentration × tissue mass)/total dose × 100%. The volumes of bile and urine at each time point were experimentally measured. The total plasma volume and tissue masses were calculated using rat body weight and previously reported rat physiological parameters[24]. The %ID of each metabolite was calculated using molar concentration. The relative abundance of each metabolite in bile and urine was calculated as: (The molar amount of individual metabolite/ the sum of molar amount of curcumin and metabolites) × 100%. WinNonlin Version 4.1 (Pharsight, Mountain View, CA) was used to calculate pharmacokinetic parameters by noncompartmental analysis.

Results

Physicochemical Characterization

We have characterized physicochemical properties of nanocurcumin including hydrodynamic size, zeta potential, and loading capacity. The intensity-weighted average hydrodynamic size of nanocurcumin was 92.4 ± 1.4 nm (Fig. S2A). The zeta potential of nanocurcumin was determined to be −20.1 ± 1.7 mV (Fig. S2B). The negative zeta potential indicated a slight net negative surface charge for the nanocurcumin. The loading capacity of curcumin was 0.93% ± 0.02% (w/w).

Stability in Buffers, Rat Plasma and Dosing Solutions

In pH 5.7 buffer, both solvent solubilized curcumin (2 μg/mL) and nanocurcumin (equivalent to 2 μg/mL curcumin) were stable (Fig. S1B). In contrast, approximately 60% of nanocurcumin and 90% of solvent solubilized curcumin decomposed after 1 h incubation in PBS (pH 7.4). Rat plasma proteins stabilized both nanocurcumin and solvent solubilized curcumin. Nanocurcumin exhibited high stability in the dosing solution (269 mg polymer/ mL, equivalent to 2.5 mg curcumin/mL, in pH 7.4 PBS), with 98.2 ± 8.8% curcumin remaining after storage at room temperature for 48 h, suggesting that the degradation rate of nanoformulated curcumin in PBS is concentration-dependent. Similarly, solvent solubilized curcumin (5 mg/mL) showed improved stability in mixed DMSO/PBS (1:1, v/v) dosing solution, with 84.2 ± 10.2% curcumin detected after 48 h storage at room temperature. To ensure there was no curcumin aggregation in the blood stream upon i.v. administration of the solvent solubilized curcumin dosing solution, the dosing solution was diluted 10, 20, and 50-fold with rat plasma. The average hydrodynamic sizes of blank rat plasma and the three diluted solutions are shown in Fig. S3. The peaks at 300 nm were likely due to the platelet-derived microparticles in rat plasma[25]. No curcumin aggregation was observed by dynamic light scattering (DLS) after 10, 20, and 50-fold dilution with rat plasma.

Plasma Concentration Profiles

Under the optimized hydrolysis assays, both glucuronides and sulfates in various matrices were completely hydrolyzed by their corresponding enzymes. The hydrolysis yields were between 80–100%. Fig. S4, for example, shows complete hydrolysis of curcumin glucuronide in bile with an average hydrolysis yield (n = 3) of 87.4 ± 5.0%.

As shown in the plasma concentration profiles, curcumin was dominant in the plasma of the nanocurcumin group (Fig. 2A) while phase II conjugates were dominant in the plasma of solvent solubilized curcumin group (Fig. 2B). The C_{max} of curcumin for the nanocurcumin group was 25.50 ± 5.94 μg/mL (n = 5), while curcumin was only detectable at 15 min for

the solvent solubilized curcumin group (14.6 ± 4.2 ng/mL, n = 5). The nanoformulation increased the plasma C_{max} of curcumin by 1749-fold. The nanoformulation also increased the plasma C_{max} of HHC conjugates and curcumin conjugates by 4.0 and 9.9-fold, respectively. THC conjugates, while present in the plasma of nanocurcumin treated animals, were not detectable for the solvent solubilized curcumin group (LOQ = 0.5 μg/mL). The curcumin Vd_{ss} for the nanocurcumin group was 320 ± 39 mL/kg (Table 1), which is much larger than the rat plasma volume of 31.2 mL/kg [24], suggesting tissue distribution or metabolism of the nanoformulated curcumin. To better understand the distribution of the nanoformulated curcumin, the plasma concentration profiles are presented as the percentage of injected dose (%ID) for each treatment group (Fig. 3). For the nanocurcumin group and solvent solubilized curcumin group, 8.0 ± 1.8% and 0.01 ± 0.01% of injected dose were detected, respectively, as curcumin in the plasma at 15 min.

Biliary Excretion

The cumulative biliary excretion of curcumin and metabolites is presented as %ID. By 1 h postdose, 17.8 ± 3.9% (Fig. 4A) and 1.6 ± 1.1% (Fig. 4B) of the injected dose was excreted into bile for nanocurcumin and solvent solubilized curcumin groups, respectively. The rapid biliary excretion of curcumin metabolites for the nanocurcumin group implied burst release of curcumin. By 8 h postdose, 25.4 ± 1.7% and 4.4 ± 1.5% of the injected dose was excreted into the bile for the nanocurcumin and solvent solubilized curcumin groups, respectively. Nanoformulation increased the total biliary excretion of curcumin and metabolites by 5.7-fold. To demonstrate the effects of nanoformulation on the metabolite profile, the relative abundance of curcumin and metabolites excreted into bile during 0 – 8 h postdose are presented in Fig. 5. Rats 1–5 were treated with nanocurcumin and rats 6–10 were treated with solvent solubilized curcumin. For both groups, the major metabolites in bile were THC and HHC conjugates (totally > 80%). Free THC and HHC were not detectable. For the solvent solubilized curcumin group, concentrations of THC glucuronides were lower than the LOQ (2 μg/mL). Nanoformulation did not change the relative abundance of sulfates or dual conjugates of curcumin, THC and HHC in bile. However, the nanoformulation increased the relative abundance of curcumin and curcumin glucuronides by 2.9 and 7.9-fold, respectively. Due to bile duct cannulation, less than 0.01% of the injected dose was detected in feces over 24 h for both groups, which might have resulted from urine contamination.

Urinary excretion

The cumulative urinary excretion of curcumin and metabolites is presented as %ID. By 8 h postdose, 2.8 ± 3.0% (Fig. 6A) and 0.2 ± 0.2% (Fig. 6B) of the injected dose was excreted into the urine for the nanocurcumin and solvent solubilized curcumin groups, respectively. In total, 28.2% and 4.7% of injected dose was excreted into bile and urine during 0–8 h postdose for the nanocurcumin and solvent solubilized curcumin groups, respectively. By 24 h postdose, 3.0 ± 3.0% and 0.4 ± 0.1% of the injected dose accumulated in urine for the nanocurcumin group and solvent solubilized curcumin group, respectively. Nanoformulation increased total urinary excretion of curcumin and metabolites by 7.1-fold. Fig. 7 shows the relative abundance of curcumin and each metabolite excreted into urine during 0 – 24 h postdose. For both the nanocurcumin group (Rats 1–5) and the solvent solubilized curcumin group (Rats 6–10), the major metabolites in urine were HHC sulfates and dual conjugates (totally > 60%). HHC glucuronides (LOQ = 1 μg/mL) and THC conjugates (LOQ = 2.5 μg/mL) were not detected in urine for the solvent solubilized curcumin group. In contrast, HHC glucuronides were detected in urine for the nanocurcumin group (1.0 ± 1.3% of total amount of curcumin and metabolites in urine). The nanoformulation decreased the relative abundance of curcumin, curcumin glucuronides, and curcumin sulfates and dual conjugates in urine by 75.9%, 81.6% and 78.1%, respectively.

Tissue Distribution

Tissue distribution data of curcumin and its metabolites for the nanocurcumin (Fig. 8A) and solvent solubilized curcumin groups (Fig. 8B) are presented as %ID. Consistent with the above main plasma PK study, 6.6 ± 0.5% and 0.05 ± 0.05% of injected dose was detected as curcumin in plasma at 15 min postdose for the nanocurcumin and solvent solubilized curcumin groups, respectively. At 15 min postdose, 0.3 ± 0.1% (nanocurcumin group) and 0.07 ± 0.006% (solvent solubilized curcumin group) of the injected dose was detected in plasma as vanillylidenacetone (degradation product of curcumin), suggesting that degradation of curcumin in the blood circulation was very limited. Vanillylidenacetone was not detected in other tissues. No significant accumulation of nanoformulated curcumin in lung, spleen, heart and kidneys was observed (Fig. 8A). Surprisingly, 58.3 ± 4.4% of the injected solvent solubilized curcumin accumulated in lung at 15 min postdose (Fig. 8B), while only 0.3 ± 0.05% of injected nanocurcumin distributed in lung at the same time point. Hence, the nanoformulation changed tissue distribution of curcumin and prevented curcumin accumulation in the lung. For both groups, HHC and THC conjugates were not detected, and curcumin was the dominate analyte in lung, spleen, heart and kidneys. In contrast, HHC conjugates were dominant in liver at 15 min postdose for both groups. Overall, the nanoformulation changed tissue distribution of curcumin and decreased the relative abundance of metabolites in plasma, but did not significantly change the relative metabolite-to-curcumin ratios in major organs.

Fig. 8 also shows the changes in curcumin concentrations in plasma, lung, liver, spleen, heart and kidneys between 15 – 60 min. For the solvent solubilized curcumin group, the dramatic decrease in curcumin concentrations in plasma, spleen, heart and kidney over the 60 min time period suggests rapid elimination of curcumin. In contrast, for the nanocurcumin group, changes in curcumin concentrations were not observed in plasma, lung, heart and kidneys, suggesting a fraction of stable nanoparticles in these organs that protected curcumin from metabolism. For the nanocurcumin group, the curcumin concentration in spleen and liver increased from 15 min to 60 min, possibly due to release of curcumin from phagocytosed nanoparticles.

Discussion

Various nanoformulations have been successfully utilized for delivery of hydrophobic drugs, increasing drug solubility and metabolic stability, while decreasing toxicity. Nanoformulations also have the potential to alter the ADME of encapsulated drugs[26], and drug release kinetics is one of the critical factors. Although polymeric nanoparticle entrapment is an attractive vehicle for curcumin delivery, rapid, “burst” drug release from polymeric nanoparticles is commonly observed in vitro[27, 28] and in vivo[29]. In this study, we evaluated the effects of polymeric nanoparticle entrapment of curcumin on plasma pharmacokinetics, metabolite profile, biliary and urinary excretion, and tissue distribution, and further utilized metabolite profiles to estimate in vivo release.

Consistent with previous nanoparticle studies[10, 30], nanocurcumin increased the plasma curcumin C_{max} by 1749-fold in comparison to solvent solubilized curcumin. The most likely explanation for the increase in nanocurcumin plasma concentration relative to solvent solubilized curcumin, is circulation of an encapsulated curcumin fraction (approx. 8% of the injected dose) which is not subjected to hepatic metabolism. Nanocurcumin also increased the plasma Cmax of phase II metabolites by 4.0 – 9.9 fold. The low amount of encapsulated curcumin in circulation coupled with the high metabolite concentrations could have several possible causes, including nanoparticle accumulation in tissues, rapid degradation of curcumin, or burst release of curcumin.

Tissue distribution studies did not reveal significant accumulation of curcumin in lung, liver, spleen, heart and kidneys 15 and 60 min postdose of nanocurcumin (Fig. 8A). Furthermore, only 0.3 ± 0.1% of administered nanoformulated curcumin decomposed into vanillylidenacetone in plasma at 15 min postdose, suggesting that the rapid elimination of nanoformulated curcumin from plasma was not due to curcumin degradation. Suggestive of burst release, biliary excretion studies showed that 17.8 ± 3.9% of the injected dose was excreted into bile mainly as metabolites at 1 h postdose. Since only released curcumin can be metabolized, the detection of significant amounts of early metabolites in bile, urine and plasma supports a burst release mechanism. Burst release of the unaccounted for nanocurcumin fraction (>90%ID) would provide high concentrations of free curcumin for hepatic metabolism. In comparison, due to accumulation of a large portion of solvent solubilized curcumin dose in tissues (i.e. ~60 % lung), a relatively smaller fraction of unaccounted for solvent solubilized curcumin (~40%) is potentially available for metabolism. Due to uncertainty in the estimation of free curcumin available for metabolism in the solvent solubilized and nanocurcumin groups, a relationship between free curcumin and metabolism data cannot be determined, and we are unable to draw conclusions regarding the absolute extent and profile of the curcumin release from nanocurcumin. However, the low amount of circulating nanocurcumin (8% ID) and relatively high plasma, biliary and urinary metabolites, suggests rapid release of a substantial fraction of the encapsulated curcumin.

The in vitro release of nanocurcumin was assessed previously in buffer (~40% release over 24h), but this system did not evaluate the interaction of the nanoparticles with blood components found in vivo[31]. In order to identify the possible influence of nanoparticle physiochemical characteristics on curcumin burst release behavior in vivo, previous reports of nanoparticle curcumin pharmacokinetics are summarized in Table 2. Consistent with our findings, low curcumin concentrations were observed following administration of PEG-PCL micelles[32], PLGA nanoparticles[16, 33, 34], D-a-tocopheryl polyethylene glycol 1000 succinate (TPGS) nanoparticles[35], polybutylcyanoacrylate nanoparticles[36], and glycerol monooleate/ pluronic F-127 nanoparticles[30] in mice, rats and rabbits. Only 1–13.4% of the dose was detected in plasma at T_{max} after i.v injection of the various curcumin-loaded nanoparticles (Table 2), regardless of particle size or charge. Most likely due to lipophilic plasma proteins, and the large membrane pool present in blood cells and tissues, it appears difficult to completely eliminate burst release from polymeric nanoparticles[22, 37–41]. However, it is possible to reduce the extent of burst release by increasing the hydrophobicity of the micelle core, decreasing drug loading, and/or improving polymer-drug compatibility[42].

After the initial burst release, the concentration of the remaining curcumin in plasma declined monoexponentially, consistent with first-order tissue uptake or slow release of the remaining encapsulated curcumin (Fig. 3). The low toxicity and rapid metabolism of curcumin and its metabolites, suggests that the possible burst release of more than 90% of curcumin dose may not impose toxic effects on off-target tissues. The prolonged circulation of the remaining encapsulated curcumin fraction could allow for tumor accumulation through the EPR effect, as shown previously for polymeric formulations[43]. This EPR accumulation of the remaining encapsulated curcumin would likely allow attainment of tumor concentrations greater than the solvent solubilized curcumin.

The altered lung and spleen distribution observed for nanocurcumin deserves further comment. Approximately 60% of the solvent solubilized curcumin accumulated in the lung, while lung accumulation of nanoformulated curcumin was not observed. Consistently, accumulation of curcumin in the lung has been reported previously in rats[44] and mice[35] following i.v. administration of free curcumin. Although solvent solubilized curcumin did not aggregate in rat plasma, curcumin may still precipitate upon interaction with red blood

cells, and these particles could then accumulate in lung due to the narrow vasculature. The time-dependent accumulation of curcumin in the spleen, observed only in the nanocurcumin group, likely resulted from phagocyte uptake of unreleased nanoparticle-entrapped curcumin.

Interestingly, nanocurcumin altered biliary and urinary metabolite profiles. Nanocurcumin exhibited higher biliary excretion of curcumin and glucuronides relative to other biliary metabolites. The increase in biliary curcumin may have resulted from saturation of the P450 enzymes following burst release. Alternatively, a previous study reported biliary excretion of 36% and 16% of parenterally administered 50 nm and 500 nm diameter polymeric nanoparticles, respectively, over a 24h period[45]. Correspondingly, biliary excretion of nanoparticles containing encapsulated curcumin might also account for the increase in the relative percentage of curcumin in bile. The increased urinary curcumin excretion for nanocurcumin is more likely due to high systemic curcumin exposure and not excretion of encapsulated curcumin, as nanoparticles with a hydrodynamic diameter over 5.5 nm are unable to be eliminated through urinary excretion[48]. Since hepatic UGTs appear to have a very high capacity for curcumin glucuronidation [46], they are less likely to be temporarily saturated by the burst released curcumin in comparison to hepatic sulfotransferases (SULTs). This might explain the increase in the relative abundance of glucuronides in bile following burst release. Indeed, in vitro studies in which curcumin was incubated with rat liver subcellular fractions at a high micromolar concentration[47], resulted in greater formation of glucuronide (980 ± 150 nmol/mg protein) than sulfate conjugates (182 ± 39 nmol/mg protein). The greater relative abundance of curcumin and curcumin conjugates in urine for solvent solubilized curcumin (Fig. 7), may simply be explained by the higher LOQ for THC in comparison to curcumin (2500 vs. 20 ng/mL, respectively) (Table S2) resulting in an inability to detect THC metabolites in the solvent solubilized curcumin group.

In summary, this study highlights the importance of in vivo drug release on the ADME of nanoformulated lipophilic drugs. Curcumin burst release from the polymeric nanoparticles increased biliary and urinary excretion of both curcumin and metabolites, but did not change the dominant elimination pathways. While nanocurcumin increased the relative abundance of curcumin and glucuronides in bile, urine and tissue metabolite profiles were not dramatically altered. Although the burst release observed in this study is a limitation for targeted tumor delivery, nanocurcumin still exhibits major advantages over solvent solubilized curcumin, as the nanoformulation does not result in lung accumulation and increases overall systemic curcumin exposure. Additionally, the remaining encapsulated curcumin fraction following burst release is available for tumor delivery via EPR.

Supplementary Material

Refer to Web version on PubMed Central for supplementary material.

Acknowledgments

The authors thank Dr. Rachael M. Crist for assistance in revising the manuscript, Ms. Sarah Skoczen for assistance with bioanalysis, and Dr. Jeffrey D. Clogston for assistance with particle size measurement. This project has been funded in whole or in part with federal funds from the National Cancer Institute, National Institutes of Health, under Contract No. HHSN261200800001E.

Abbreviations

MPS	mononuclear phagocytic system
AUC	Area under the curve

Cmax	concentration maximum
EPR	enhanced permeability and retention
THC	tetrahydrocurcumin
HHC	hydrotetracurcumin
MRT	mean residence time
%ID	percentage of injected dose
NIPAAM	N-isopropylacrylamide
VP	vinylpyrrolidone
AA	acrylic acid
IS	internal standard
LOQ	limit of quantitation
S/N	signal-to-noise
UGT	UDP-glucuronosyltransferase
SULT	sulfotransferase
ADME	absorption, distribution, metabolism, and excretion

References

1. Kadam RS, Bourne DW, Kompella UB. Nano-advantage in enhanced drug delivery with biodegradable nanoparticles: contribution of reduced clearance. Drug metabolism and disposition: the biological fate of chemicals. 2012; 40(7):1380–8. [PubMed: 22498894]
2. Stern ST, Hall JB, Yu LL, Wood LJ, Paciotti GF, Tamarkin L, Long SE, McNeil SE. Translational considerations for cancer nanomedicine. Journal of controlled release : official journal of the Controlled Release Society. 2010; 146(2):164–74. [PubMed: 20385183]
3. Bui T, Stevenson J, Hoekman J, Zhang S, Maravilla K, Ho RJ. Novel Gd nanoparticles enhance vascular contrast for high-resolution magnetic resonance imaging. PloS one. 2010; 5(9)
4. Parker RJ, Priester ER, Sieber SM. Effect of route administration and liposome entrapment on the metabolism and disposition of adriamycin in the rat. Drug metabolism and disposition: the biological fate of chemicals. 1982; 10(5):499–504. [PubMed: 6128200]
5. van Borssum Waalkes M, Kuipers F, Havinga R, Scherphof GL. Conversion of liposomal 5-fluoro-2′-deoxyuridine and its dipalmitoyl derivative to bile acid conjugates of alpha-fluoro-beta-alanine and their excretion into rat bile. Biochimica et biophysica acta. 1993; 1176(1–2):43–50. [PubMed: 8452878]
6. Hu CM, Zhang L, Aryal S, Cheung C, Fang RH, Zhang L. Erythrocyte membrane-camouflaged polymeric nanoparticles as a biomimetic delivery platform. Proceedings of the National Academy of Sciences of the United States of America. 2011; 108(27):10980–5. [PubMed: 21690347]
7. Hrkach J, Von Hoff D, Mukkaram Ali M, Andrianova E, Auer J, Campbell T, De Witt D, Figa M, Figueiredo M, Horhota A, Low S, McDonnell K, Peeke E, Retnarajan B, Sabnis A, Schnipper E, Song JJ, Song YH, Summa J, Tompsett D, Troiano G, Van Geen Hoven T, Wright J, LoRusso P, Kantoff PW, Bander NH, Sweeney C, Farokhzad OC, Langer R, Zale S. Preclinical development and clinical translation of a PSMA-targeted docetaxel nanoparticle with a differentiated pharmacological profile. Science translational medicine. 2012; 4(128):128ra39.
8. Ding XY, Hong CJ, Liu Y, Gu ZL, Xing KL, Zhu AJ, Chen WL, Shi LS, Zhang XN, Zhang Q. Pharmacokinetics, tissue distribution, and metabolites of a polyvinylpyrrolidone-coated norcantharidin chitosan nanoparticle formulation in rats and mice, using LC-MS/MS. International journal of nanomedicine. 2012; 7:1723–35. [PubMed: 22619523]

9. Yallapu MM, Jaggi M, Chauhan SC. Curcumin nanoformulations: a future nanomedicine for cancer. Drug discovery today. 2012; 17(1–2):71–80. [PubMed: 21959306]
10. Bisht S, Mizuma M, Feldmann G, Ottenhof NA, Hong SM, Pramanik D, Chenna V, Karikari C, Sharma R, Goggins MG, Rudek MA, Ravi R, Maitra A, Maitra A. Systemic administration of polymeric nanoparticle-encapsulated curcumin (NanoCurc) blocks tumor growth and metastases in preclinical models of pancreatic cancer. Molecular cancer therapeutics. 2010; 9(8):2255–64. [PubMed: 20647339]
11. Pramanik D, Campbell NR, Das S, Gupta S, Chenna V, Bisht S, Sysa-Shah P, Bedja D, Karikari C, Steenbergen C, Gabrielson KL, Maitra A, Maitra A. A composite polymer nanoparticle overcomes multidrug resistance and ameliorates doxorubicin-associated cardiomyopathy. Oncotarget. 2012; 3(6):640–50. [PubMed: 22791660]
12. Wang YJ, Pan MH, Cheng AL, Lin LI, Ho YS, Hsieh CY, Lin JK. Stability of curcumin in buffer solutions and characterization of its degradation products. Journal of pharmaceutical and biomedical analysis. 1997; 15(12):1867–76. [PubMed: 9278892]
13. Vareed SK, Kakarala M, Ruffin MT, Crowell JA, Normolle DP, Djuric Z, Brenner DE. Pharmacokinetics of curcumin conjugate metabolites in healthy human subjects. Cancer epidemiology, biomarkers & prevention : a publication of the American Association for Cancer Research, cosponsored by the American Society of Preventive Oncology. 2008; 17(6):1411–7.
14. Pan MH, Huang TM, Lin JK. Biotransformation of curcumin through reduction and glucuronidation in mice. Drug metabolism and disposition: the biological fate of chemicals. 1999; 27(4):486–94. [PubMed: 10101144]
15. Bansal SS, Goel M, Aqil F, Vadhanam MV, Gupta RC. Advanced drug delivery systems of curcumin for cancer chemoprevention. Cancer prevention research. 2011; 4(8):1158–71. [PubMed: 21546540]
16. Tsai YM, Chien CF, Lin LC, Tsai TH. Curcumin and its nano-formulation: the kinetics of tissue distribution and blood-brain barrier penetration. International journal of pharmaceutics. 2011; 416(1):331–8. [PubMed: 21729743]
17. Cartiera MS, Ferreira EC, Caputo C, Egan ME, Caplan MJ, Saltzman WM. Partial correction of cystic fibrosis defects with PLGA nanoparticles encapsulating curcumin. Molecular pharmaceutics. 2010; 7(1):86–93. [PubMed: 19886674]
18. Shahani K, Swaminathan SK, Freeman D, Blum A, Ma L, Panyam J. Injectable sustained release microparticles of curcumin: a new concept for cancer chemoprevention. Cancer research. 2010; 70(11):4443–52. [PubMed: 20460537]
19. Onoue S, Takahashi H, Kawabata Y, Seto Y, Hatanaka J, Timmermann B, Yamada S. Formulation design and photochemical studies on nanocrystal solid dispersion of curcumin with improved oral bioavailability. Journal of pharmaceutical sciences. 2010; 99(4):1871–81. [PubMed: 19827133]
20. Murugan P, Pari L. Effect of tetrahydrocurcumin on plasma antioxidants in streptozotocin-nicotinamide experimental diabetes. Journal of basic and clinical physiology and pharmacology. 2006; 17(4):231–44. [PubMed: 17338279]
21. Pfeiffer E, Hoehle SI, Walch SG, Riess A, Solyom AM, Metzler M. Curcuminoids form reactive glucuronides in vitro. Journal of agricultural and food chemistry. 2007; 55(2):538–44. [PubMed: 17227090]
22. Letchford K, Burt HM. Copolymer micelles and nanospheres with different in vitro stability demonstrate similar paclitaxel pharmacokinetics. Molecular pharmaceutics. 2012; 9(2):248–60. [PubMed: 22204437]
23. Bisht S, Feldmann G, Koorstra JB, Mullendore M, Alvarez H, Karikari C, Rudek MA, Lee CK, Maitra A, Maitra A. In vivo characterization of a polymeric nanoparticle platform with potential oral drug delivery capabilities. Molecular cancer therapeutics. 2008; 7(12):3878–88. [PubMed: 19074860]
24. Davies B, Morris T. Physiological parameters in laboratory animals and humans. Pharmaceutical research. 1993; 10(7):1093–5. [PubMed: 8378254]
25. Li X, Cong H. Platelet-derived microparticles and the potential of glycoprotein IIb/IIIa antagonists in treating acute coronary syndrome. Texas Heart Institute journal/from the Texas Heart Institute of St Luke's Episcopal Hospital, Texas Children's Hospital. 2009; 36(2):134–9.

26. Guidance for industry: liposome drug products. U.S. Food and Drug Administration; Rockville, MD: 2002.
27. Zhang L, Hu Y, Jiang X, Yang C, Lu W, Yang YH. Camptothecin derivative-loaded poly(caprolactone-co-lactide)-b-PEG-b-poly(caprolactone-co-lactide) nanoparticles and their biodistribution in mice. Journal of controlled release : official journal of the Controlled Release Society. 2004; 96(1):135–48. [PubMed: 15063036]
28. Danhier F, Lecouturier N, Vroman B, Jerome C, Marchand-Brynaert J, Feron O, Preat V. Paclitaxel-loaded PEGylated PLGA-based nanoparticles: in vitro and in vivo evaluation. Journal of controlled release : official journal of the Controlled Release Society. 2009; 133(1):11–7. [PubMed: 18950666]
29. Ma X, Oyamada S, Gao F, Wu T, Robich MP, Wu H, Wang X, Buchholz B, McCarthy S, Gu Z, Bianchi CF, Sellke FW, Laham R. Paclitaxel/sirolimus combination coated drug-eluting stent: in vitro and in vivo drug release studies. Journal of pharmaceutical and biomedical analysis. 2011; 54(4):807–11. [PubMed: 21126843]
30. Mohanty C, Sahoo SK. The in vitro stability and in vivo pharmacokinetics of curcumin prepared as an aqueous nanoparticulate formulation. Biomaterials. 2010; 31(25):6597–611. [PubMed: 20553984]
31. Bisht S, Feldmann G, Soni S, Ravi R, Karikar C, Maitra A, Maitra A. Polymeric nanoparticle-encapsulated curcumin ("nanocurcumin"): a novel strategy for human cancer therapy. Journal of nanobiotechnology. 2007; 5:3. [PubMed: 17439648]
32. Gou M, Men K, Shi H, Xiang M, Zhang J, Song J, Long J, Wan Y, Luo F, Zhao X, Qian Z. Curcumin-loaded biodegradable polymeric micelles for colon cancer therapy in vitro and in vivo. Nanoscale. 2011; 3(4):1558–67. [PubMed: 21283869]
33. Tsai YM, Jan WC, Tsai TH. Optimised nano-formulation on the bioavailability of hydrophobic polyphenol, curcumin, in freely-moving rats. Food Chemistry. 2011; 127:918–925.
34. Song Z, Feng R, Sun M, Guo C, Gao Y, Li L, Zhai G. Curcumin-loaded PLGA-PEG-PLGA triblock copolymeric micelles: Preparation, pharmacokinetics and distribution in vivo. Journal of colloid and interface science. 2011; 354(1):116–23. [PubMed: 21044788]
35. Gao Y, Li Z, Sun M, Li H, Guo C, Cui J, Li A, Cao F, Xi Y, Lou H, Zhai G. Preparation, characterization, pharmacokinetics, and tissue distribution of curcumin nanosuspension with TPGS as stabilizer. Drug development and industrial pharmacy. 2010; 36(10):1225–34. [PubMed: 20545506]
36. Sun M, Gao Y, Guo C, Zhai G. Enhancement of transport of curcumin to brain in mice by poly(n-butylcyanoacrylate) nanoparticle. Journal of Nanoparticle Research. 2010; 12:3111–3122.
37. Kim SC, Kim DW, Shim YH, Bang JS, Oh HS, Wan Kim S, Seo MH. In vivo evaluation of polymeric micellar paclitaxel formulation: toxicity and efficacy. J Control Release. 2001; 72(1–3): 191–202. [PubMed: 11389998]
38. Chen H, Kim S, He W, Wang H, Low PS, Park K, Cheng JX. Fast release of lipophilic agents from circulating PEG-PDLLA micelles revealed by in vivo forster resonance energy transfer imaging. Langmuir. 2008; 24(10):5213–7. [PubMed: 18257595]
39. Kim S, Shi Y, Kim JY, Park K, Cheng JX. Overcoming the barriers in micellar drug delivery: loading efficiency, in vivo stability, and micelle-cell interaction. Expert Opin Drug Deliv. 2010; 7(1):49–62. [PubMed: 20017660]
40. Xu P, Gullotti E, Tong L, Highley CB, Errabelli DR, Hasan T, Cheng JX, Kohane DS, Yeo Y. Intracellular drug delivery by poly(lactic-co-glycolic acid) nanoparticles, revisited. Mol Pharm. 2009; 6(1):190–201. [PubMed: 19035785]
41. Liu J, Zeng F, Allen C. Influence of serum protein on polycarbonate-based copolymer micelles as a delivery system for a hydrophobic anti-cancer agent. J Control Release. 2005; 103(2):481–97. [PubMed: 15763628]
42. Liu J, Lee H, Allen C. Formulation of drugs in block copolymer micelles: drug loading and release. Current pharmaceutical design. 2006; 12(36):4685–701. [PubMed: 17168772]
43. Schluep T, Hwang J, Hildebrandt IJ, Czernin J, Choi CH, Alabi CA, Mack BC, Davis ME. Pharmacokinetics and tumor dynamics of the nanoparticle IT-101 from PET imaging and tumor

histological measurements. Proceedings of the National Academy of Sciences of the United States of America. 2009; 106(27):11394–9. [PubMed: 19564622]

44. Jiang, F.; Yu, T.; Liu, X. Biodistribution of curcumin and its derivatives new aspects for curcumin administration. International Conference on Remote Sensing, Environment and Transportation Engineering (RSETE); Nanjing, China. 2011; July 24–26;
45. Jani PU, Nomura T, Yamashita F, Takakura Y, Florence AT, Hashida M. Biliary excretion of polystyrene microspheres with covalently linked FITC fluorescence after oral and parenteral administration to male Wistar rats. Journal of drug targeting. 1996; 4(2):87–93. [PubMed: 8894968]
46. Hoehle SI, Pfeiffer E, Metzler M. Glucuronidation of curcuminoids by human microsomal and recombinant UDP-glucuronosyltransferases. Molecular nutrition & food research. 2007; 51(8): 932–8. [PubMed: 17628876]
47. Ireson CR, Jones DJ, Orr S, Coughtrie MW, Boocock DJ, Williams ML, Farmer PB, Steward WP, Gescher AJ. Metabolism of the cancer chemopreventive agent curcumin in human and rat intestine. Cancer epidemiology, biomarkers & prevention : a publication of the American Association for Cancer Research, cosponsored by the American Society of Preventive Oncology. 2002; 11(1):105–11.
48. Moghimi SM, Hunter AC, Andresen TL. Factors controlling nanoparticle pharmacokinetics: an integrated analysis and perspective. Annual review of pharmacology and toxicology. 2012; 52:481–503.

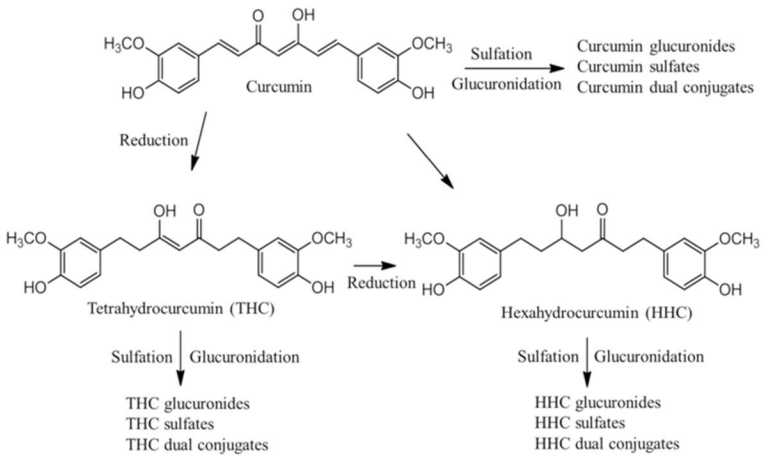

Figure 1.
Metabolic pathways of curcumin in rats.

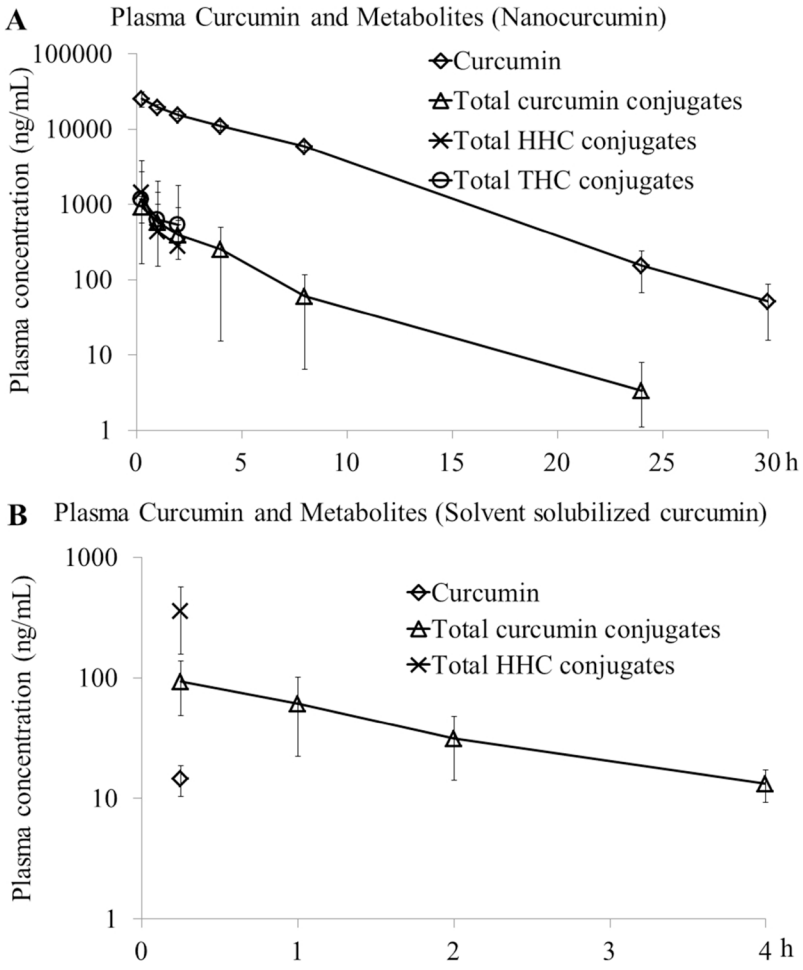

Figure 2.

Plasma concentration-time profiles of curcumin and its metabolites after i.v. administration of (A) nanocurcumin (equivalent to 10 mg/kg curcumin) and (B) solvent solubilized curcumin (10 mg/kg) to SD rats. Each point represents the mean ± S.D. from n = 5 rats. For the nanocurcumin group, the plasma concentrations of THC conjugates and HHC conjugates were lower than the LOQs 4 h post dose. For the solvent solubilized curcumin group, the plasma concentrations of HHC conjugates and curcumin were lower than the LOQs 1 h postdose, and the plasma concentrations of curcumin conjugates were lower than the LOQ 8 h postdose. THC conjugates were not detectable in the plasma samples of the solvent solubilized curcumin group.

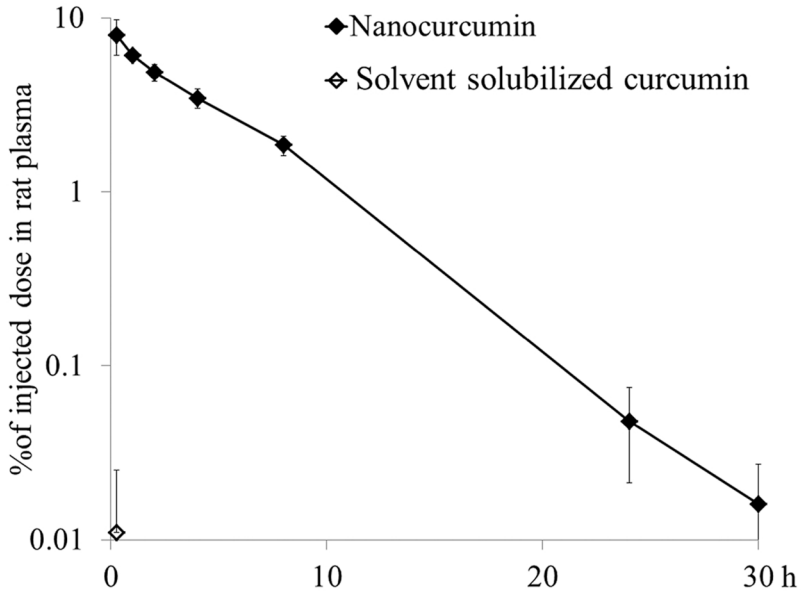

Figure 3.

Plasma concentration-time profiles of curcumin presented as the percentage of injected dose (%ID) after i.v. administration of nanocurcumin (equivalent to 10 mg/kg curcumin) and solvent solubilized curcumin (10 mg/kg) to SD rats. Each point represents the mean ± S.D. from n = 5 rats. The %ID of curcumin in plasma was calculated as: (curcumin concentration × total plasma volume)/total dose × 100%.

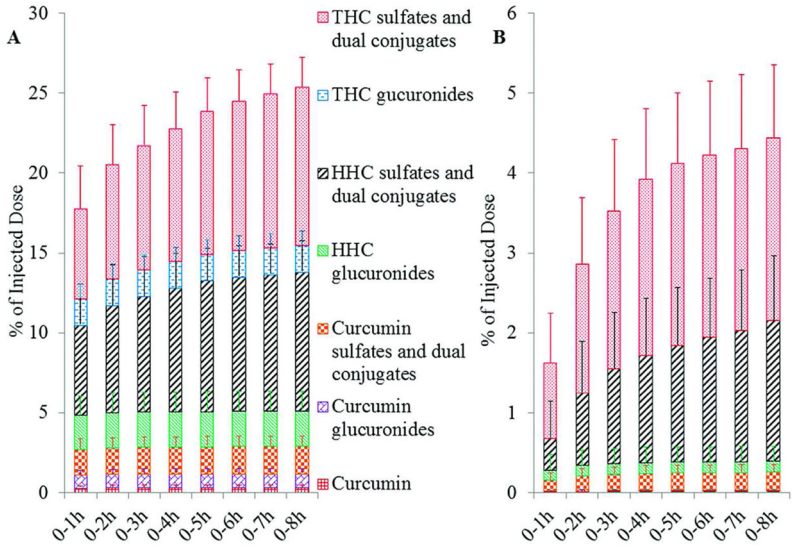

Figure 4.

Cumulative biliary excretion of curcumin and its metabolites after i.v. administration of (A) nanocurcumin (equivalent to 10 mg/kg curcumin) and (B) solvent solubilized curcumin (10 mg/kg) to SD rats. Data are mean ± S.D., n = 5 rats. Bile samples were collected at 1 h intervals for the first 8 h. The %ID of curcumin and metabolites in bile was calculated as: (curcumin or metabolite molar concentration × volume of collected bile)/total molar dose × 100%.

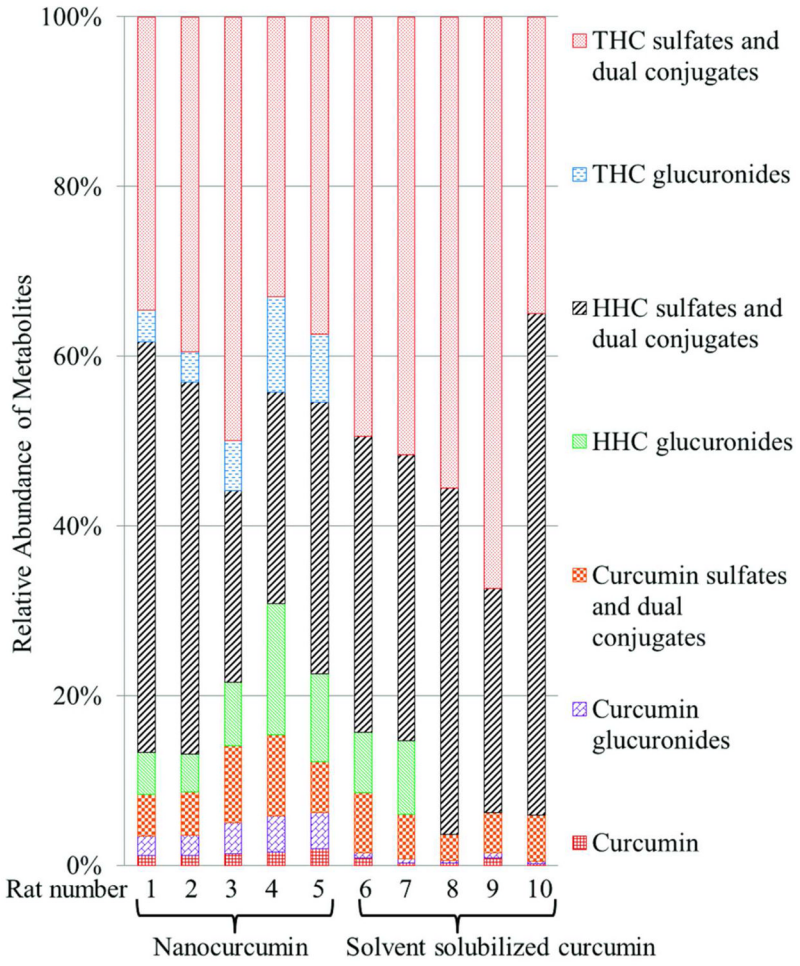

Figure 5.

Relative abundance of curcumin and its metabolites excreted into bile 0–8 h post i.v. administration of nanocurcumin (equivalent to 10 mg/kg curcumin) to rat 1–5 and solvent solubilized curcumin (10 mg/kg) to rat 6–10. The relative abundance of curcumin or metabolites in bile was calculated as: (The molar amount of curcumin or individual metabolite in bile/the sum of molar amount of curcumin and metabolites in bile) × 100%.

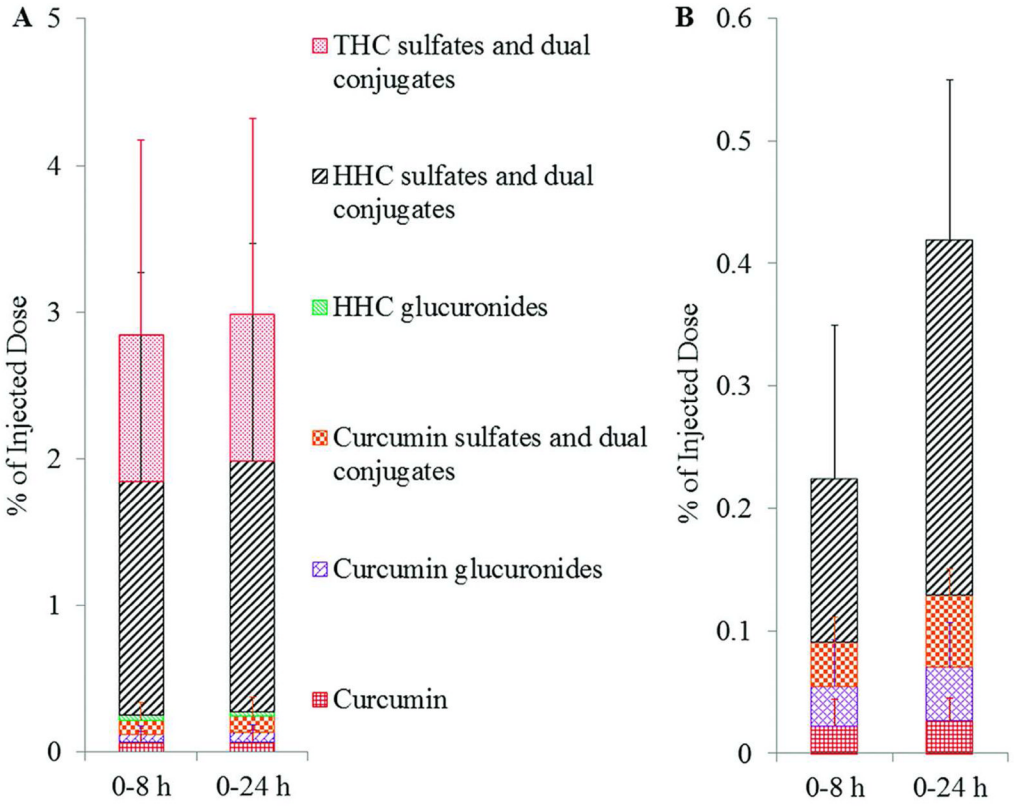

Figure 6.

Cumulative urinary excretion of curcumin and its metabolites after i.v. administration of (A) nanocurcumin (equivalent to 10 mg/kg curcumin) and (B) solvent solubilized curcumin (10 mg/kg) to SD rats. Data are mean ± S.D., n = 5 rats. Urine samples were collected at 0–8 and 8–24 h intervals. The %ID of curcumin and metabolites in bile was calculated as: (curcumin or metabolite molar concentration × volume of collected urine)/total molar dose × 100%.

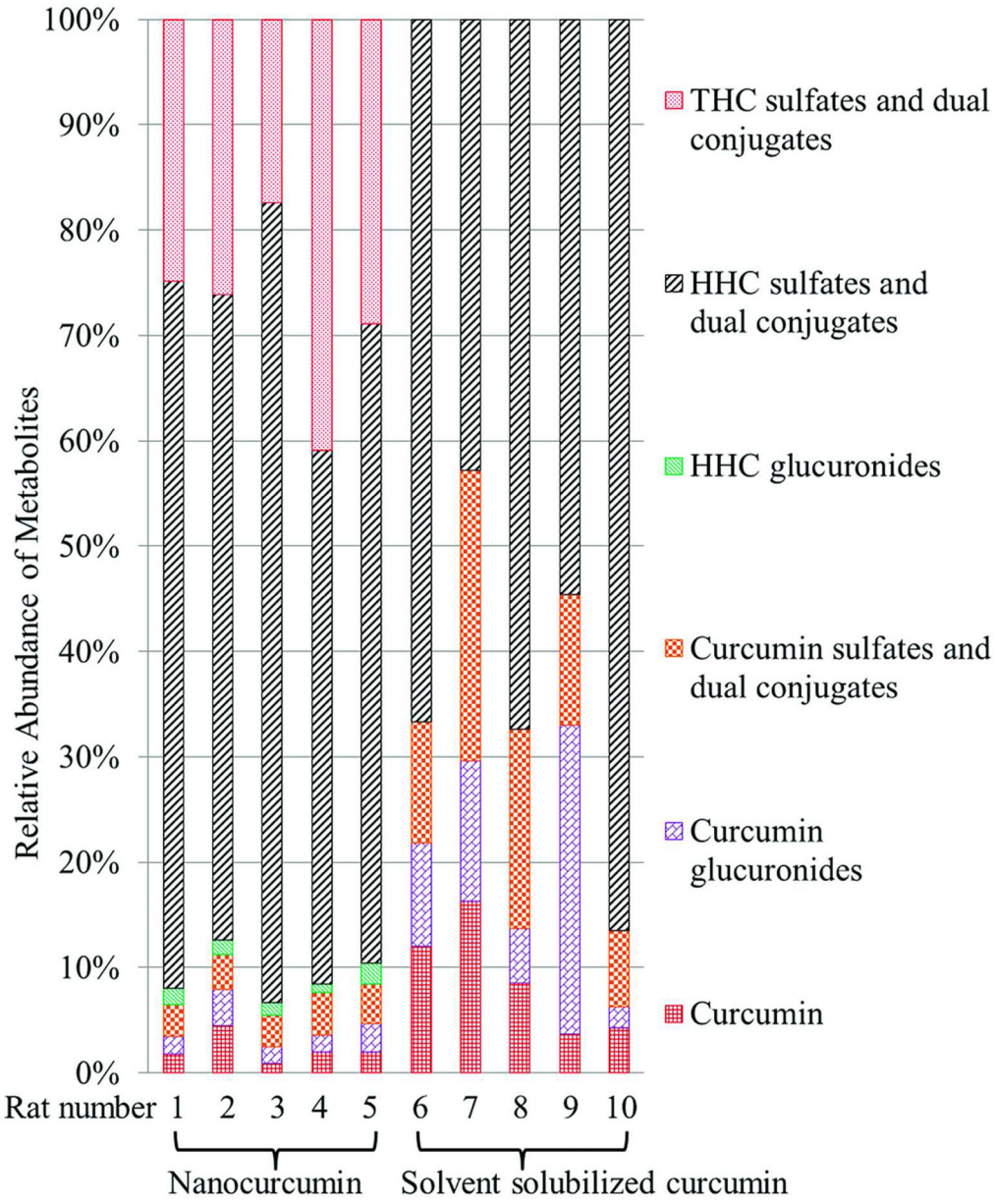

Figure 7.

Relative abundance of curcumin and its metabolites excreted into urine 0–24 h post i.v. administration of nanocurcumin (equivalent to 10 mg/kg curcumin) to rat 1–5 and solvent solubilized curcumin (10 mg/kg) to rat 6–10. The relative abundance of curcumin or metabolites in urine was calculated as: (The molar amount of curcumin or individual metabolite in urine/the sum molar amount of curcumin and metabolites in urine) × 100%.

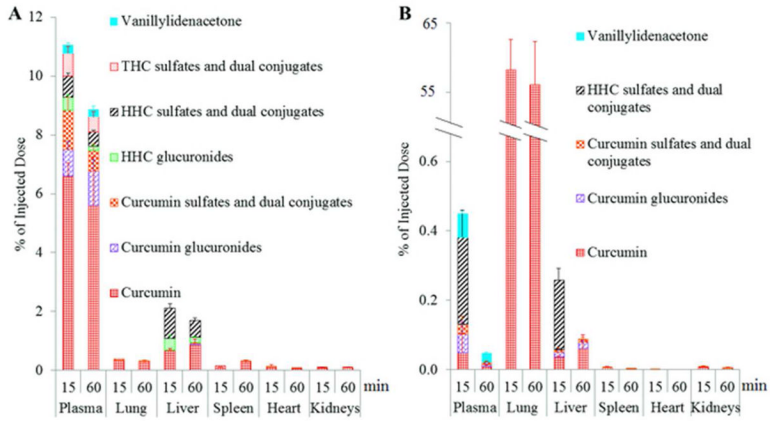

Figure 8.

Biodistribution of curcumin and its metabolites 15 min and 60 min post i.v. administration of (A) nanocurcumin (equivalent to 10 mg/kg curcumin) and (B) solvent solubilized curcumin (10 mg/kg) to SD rats. Data are mean ± S.D., n = 3 rats. Plasma and tissue samples were collected at 15 min and 60 min postdose. The %ID of curcumin and metabolites in plasma was calculated as: (curcumin or metabolite molar concentration × total plasma volume)/total molar dose × 100%. The %ID of curcumin and metabolites in tissues was calculated as: (curcumin or metabolite molar concentration × tissue mass)/total molar dose × 100%.

Table 1

Pharmacokinetic parameters of nanocurcumin in SD rats (n =5) derived by noncompartmental analysis

PK parameters	nanocurumin group
CL (mL/h/kg)	66 ± 7
AUC (h*ng/mL)	151135 ± 14106
MRT (h)	4.82 ± 0.35
$T_{1/2}$ (h)	3.19 ± 0.46
Vd_{ss} (mL/kg)	320 ± 39
C_{max} (ng/mL)	25499 ± 5937

Table 2

Summary of Curcumin Nanoformulation Pharmacokinetics

Nanoparticles	DLS Size (nm)	Zeta potential (mV)	Loading capacity (%)	Dose (mg/kg)	Species	Plasma volume[#] (mL/kg)	T_{max} (min)	C_{max} (μg/mL)	% of dose in plasma at T_{max}[##]	Ref
PEG-PCL	27.3	N.A.	12.95	100	rat	31.2	5	430	13.4	32
PLGA	163	−12.5	4.69	25	rat	31.2	15	16	2.0	16
TPGS[*]	210	−14.8	N.A.	15	rabbit	44	5	25.5	7.5	35
PLGA/PVA[**]	317	−24.2	1.54	2.5	rat	31.2	5	0.83	1.0	33
Polybutylcyanoacrylate	152	0	21.1	5	mouse	50	5	1.28	1.3	36
PLGA-PEG-PLGA	26.3	−0.71	6.40	10	mouse	50	5	2.17	1.1	34
GMO[***]/pluronic F-127	192	−32	0.67	30	mouse	50	60	25	4.2	30
NIPAAM/VP/AA	92.4	−20.1	0.93	10	rat	31.2	15	25.5	8.0	This study

[*] TPGS: D-α-tocopheryl polyethylene glycol-succinate

[**] PVA: poly (vinyl alcohol)

[***] GMO: glycerol monooleate

[#] Plasma volumes of mouse, rat, and rabbit were collected from literature[24].

[##] % of dose in plasma at T_{max} = [C_{max} (mg/mL) × Plasma Volume (mL/kg)] ÷ Dose (mg/kg) × 100%